

# Textual Knowledge Matters: Cross-Modality Co-Teaching for Generalized Visual Class Discovery

Haiyang Zheng<sup>1\*</sup> Nan Pu<sup>2\*</sup> Wenjing Li<sup>3</sup> Nicu Sebe<sup>2</sup> Zhun Zhong<sup>4</sup>

<sup>1</sup> Harbin Institute of Technology, Shenzhen <sup>2</sup> University of Trento

<sup>3</sup> University of Leeds <sup>4</sup> University of Nottingham

## Abstract

In this paper, we study the problem of Generalized Category Discovery (GCD), which aims to cluster unlabeled data from both known and unknown categories using the knowledge of labeled data from known categories. Current GCD methods rely on only visual cues, which however neglect the multi-modality perceptive nature of human cognitive processes in discovering novel visual categories. To address this, we propose a two-phase TextGCD framework to accomplish multi-modality GCD by exploiting powerful Visual-Language Models. TextGCD mainly includes a retrieval-based text generation (RTG) phase and a cross-modality co-teaching (CCT) phase. First, RTG constructs a visual lexicon using category tags from diverse datasets and attributes from Large Language Models, generating descriptive texts for images in a retrieval manner. Second, CCT leverages disparities between textual and visual modalities to foster mutual learning, thereby enhancing visual GCD. In addition, we design an adaptive class aligning strategy to ensure the alignment of category perceptions between modalities as well as a soft-voting mechanism to integrate multi-modality cues. Experiments on eight datasets show the large superiority of our approach over state-of-the-art methods. Notably, our approach outperforms the best competitor, by 7.7% and 10.8% in All accuracy on ImageNet-1k and CUB, respectively.

## 1 Introduction

Despite the remarkable advancements of deep learning in visual recognition, a notable criticism is that the models, once trained, show a significant limitation in recognizing novel classes not encountered during the supervised training phase. Drawing inspiration from the innate human capacity to seamlessly acquire new knowledge with reference to previously assimilated information, Generalized Category Discovery (GCD) [Vaze et al. \(2022\)](#) is proposed to leverage the knowledge of labeled data from known categories to automatically cluster unlabeled data that belong to both known and unknown categories. While current GCD methods [Vaze et al. \(2022\)](#); [Wen et al. \(2023\)](#); [Pu et al. \(2023\)](#); [Zhao et al. \(2023\)](#); [Zhang et al. \(2023\)](#) have demonstrated considerable success utilizing advanced large-scale visual models (*e.g.*, ViT [Dosovitskiy et al. \(2020\)](#)), as illustrated in Fig. 1, they predominantly focus on visual cues. In contrast, human cognitive processes for identifying novel visual categories usually incorporate multiple modalities [Sloutsky \(2010\)](#), such as encompassing visual, auditory, and textual elements in recognizing a subject. In the light of this, unlike existing GCD methods [Vaze et al. \(2022\)](#); [Wen et al. \(2023\)](#); [Pu et al. \(2023\)](#); [Zhao et al. \(2023\)](#); [Zhang et al. \(2023\)](#); [Wang et al. \(2023\)](#) that rely on only visual modality, we propose to exploit both visual and textual cues for GCD.

In this paper, we advocate the utilization of large-scale pre-trained Visual-Language Models (VLMs) [Radford et al. \(2021\)](#); [Yu et al. \(2022\)](#); [Li et al. \(2023b\)](#) to inject rich textual information into GCD. However, VLMs

---

\* Equal Contribution.

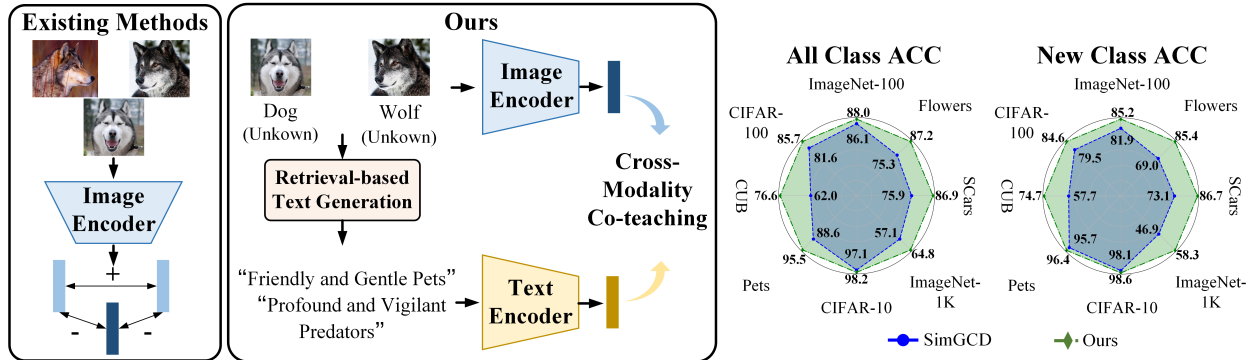


Figure 1: Left: Comparison to existing methods. Our approach introduces textual modality information (e.g., “Friendly and Gentle Pets” for Husky dogs, “Profound and Vigilant Predators” for wolves) into the framework and proposes cross-modal co-teaching for accurate generalized category discovery. Right: Performance comparison with SOTA.

require predetermined, informative textual descriptors (e.g., class names) for matching or recognizing images. This poses a significant challenge in GCD involving unlabeled data, particularly for unknown categories that lack predefined class names. Hence, how to provide relevant textual cues for unlabeled data is of a key in facilitating GCD with textual information.

To this end, we introduce the TextGCD framework, comprising a retrieval-based text generation (RTG) phase and a cross-modality co-teaching (CCT) phase, to fully leverage the mutual benefit of visual and textual cues for solving GCD. In particular, RTG initially constructs a visual lexicon encompassing category tags from diverse datasets and attributes gleaned from Large Language Models (LLMs), which offer categorical insights. Subsequently, the most pertinent tags and attributes are selected from the lexicon to craft descriptive texts for all images through an offline procedure. While the augmentation of textual information for unlabeled images via RTG is beneficial, the effective integration of this textual information to enhance visual category discovery remains an essential challenge.

To solve the challenge, we introduce CCT to leverage the inherent disparities between textual and visual modalities, harnessing these distinctions to facilitate joint learning, which is important for co-teaching Han et al. (2018). To this end, we devise a cross-modal co-teaching training strategy that fosters mutual learning and collective enhancement between text and image models. Additionally, to ensure the effective alignment of category perceptions between text and image models and to facilitate comprehensive learning from both modalities, we introduce a warm-up stage and a class-aligning stage before engaging in cross-modality co-teaching. Finally, a soft-voting mechanism is deployed to amalgamate insights from both modalities, aiming to enhance the accuracy of category determination. In short, introducing the textual modality and exchanging insights between modalities have significantly improved the precision of visual category identification, particularly for previously unseen categories. Our contributions are summarized as follows:

- We identify the limitations of existing GCD methods that rely on only visual cues and introduce additional textual information through a customized RTG based on large-scale VLMs.
- We propose a co-teaching strategy between textual and visual modalities, along with inter-modal information fusion, to fully exploit the strengths of different modalities in category discovery.

- Comprehensive experiments on eight datasets demonstrate the effectiveness of the proposed method. Notably, compared to the leading competitor in terms of All accuracy, our approach achieves an increase of 7.7% on ImageNet-1k and 10.8% on CUB. The source code will be publicly available.

## 2 Related Work

**Generalized Category Discovery (GCD)** aims to accurately classify an unlabeled set containing both known and unknown categories, based on another dataset labeled with only known categories. Vaze et al. [Vaze et al. \(2022\)](#) first proposed optimizing image feature similarities through supervised and self-supervised contrastive learning to address GCD. Building on this, SimGCD [Wen et al. \(2023\)](#) designed a parametric classification baseline for GCD. For better image representations, DCCL [Pu et al. \(2023\)](#) proposed a novel approach to contrastive learning at both the concept and instance levels. Similarly focusing on image representation, PromptCAL [Zhang et al. \(2023\)](#) introduced a Contrastive Affinity Learning approach with auxiliary visual prompts designed to amplify the semantic discriminative power of the pre-trained backbone. Furthermore, SPTNet [Wang et al. \(2023\)](#) proposed iteratively implementing model finetuning and prompt learning, resulting in clearer boundaries between different semantic categories. Unlike existing methods that primarily focus on visual cues, we design a retrieval-based approach to introduce text cues from LLM for unknown categories. Recently, CLIP-GCD [Ouldnooghi et al. \(2023\)](#) concatenated image features with textual features obtained from a Knowledge Database and categorized them using a clustering method. Unlike CLIP-GCD, which merely concatenates text and visual features from a frozen backbone, we leverage the differences between textual and visual models to establish a dynamic co-teaching scheme.

**Visual-Language Models (VLMs)** are designed to map images and text into a unified embedding space, facilitating cross-modal alignment. Among the prominent works, CLIP [Radford et al. \(2021\)](#) employs contrastive representation learning with extensive image-text pairs, showcasing remarkable zero-shot transfer capabilities across a variety of downstream tasks. Additionally, LENS [Berrios et al. \(2023\)](#) leverages VLMs as visual reasoning modules, integrating them with Large Language Models (LLMs) for diverse visual applications. As VLMs effectively bridge the visual and textual modalities, enhancing image classification tasks with knowledge from LLMs has been extensively explored [Menon & Vondrick \(2022\)](#); [Yang et al. \(2023\)](#); [Novack et al. \(2023\)](#). However, these works use VLMs to enhance image classification in scenarios where the names of all classes are predefined for VLMs. In this paper, we exploit VLMs to address the GCD task, where the unlabeled data do not have exploitable textual information for VLMs. We utilize a retrieval-based text generation method to enable the GCD task to benefit from large VLMs.

**Co-teaching** was originally proposed as a learning paradigm to address the issue of label noise [Han et al. \(2018\)](#). This strategy involves training two peer networks that select low-loss instances from a noisy mini-batch to train each other. Nested-Co-teaching [Chen et al. \(2021\)](#) and JoCoR [Wei et al. \(2020\)](#) further introduce compression regularization and co-regularization for each training example to optimize the co-teaching process. Yuan et al. [Yuan et al. \(2024\)](#) established three symmetric peer proxies with pseudo-label-driven co-teaching to address the Offline model-based optimization task. Yang et al. [Yang et al. \(2020\)](#) were the first to introduce the co-teaching strategy into the Person re-identification task, designing an asymmetric co-teaching framework. Similarly, Roy et al. [Roy et al. \(2021\)](#) pioneered co-teaching between classifiers of a dual classifier head to tackle the multi-target domain task. Unlike these works, our focus is on applying co-teaching to the GCD task. Furthermore, rather than employing two peer networks within the same modality or learning from self-discrepancy, we initiate co-teaching between the image model and the text model,

leveraging the disparities between modalities to foster mutual enhancement.

### 3 Method

**Task Configuration:** In GCD, we are given a labeled dataset, denoted as  $\mathcal{D}_L = \{(\mathbf{x}_i, y_i^l)\}_{i=1}^M \subseteq \mathcal{X} \times \mathcal{Y}_L$ , and an unlabeled dataset, denoted as  $\mathcal{D}_U = \{(\mathbf{x}_i, y_i^u)\}_{i=1}^N \subseteq \mathcal{X} \times \mathcal{Y}_U$ , where  $M$  and  $N$  indicate the number of samples in the  $\mathcal{D}_L$  and  $\mathcal{D}_U$ , respectively.  $\mathcal{Y}_L$  and  $\mathcal{Y}_U$  indicate the label spaces for labeled and unlabeled datasets, respectively, where  $\mathcal{Y}_L \subseteq \mathcal{Y}_U$ . That is,  $\mathcal{D}_U$  contains data from unknown categories, and  $\mathcal{Y}_U$  is unavailable. The objective of GCD is to leverage the prior knowledge from known categories within  $\mathcal{D}_L$  to classify samples in  $\mathcal{D}_U$  effectively. Following Wen et al. (2023), it is assumed that the number of classes in  $\mathcal{D}_U$ , represented by  $K = |\mathcal{Y}_U|$ , is predetermined.

#### 3.1 Overview

The framework of the proposed TextGCD, depicted in Fig. 2, consists of the Retrieval-based Text Generation (RTG) phase and Cross-modal Co-Teaching (CCT) phase. In RTG, we initially develop a visual lexicon comprising a broad spectrum of tags, along with attributes obtained from LLMs. Subsequently, we extract representations of images and the visual lexicon with an auxiliary VLM model and generate textual category information for each image in a retrieval manner. Building upon this, we design textual and visual parametric classifiers and propose the CCT phase to foster mutual learning and collective progress between text and image models.

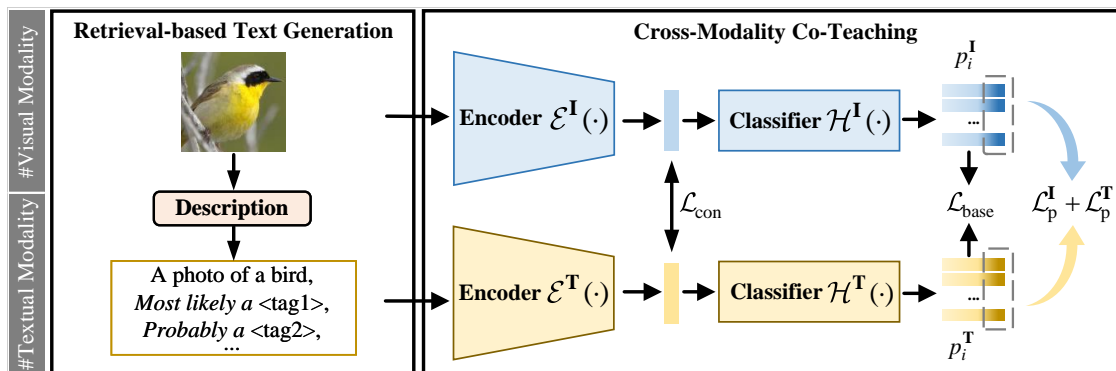


Figure 2: The TextGCD framework comprises two main phases: Retrieval-based Text Generation (RTG) and Cross-modality Co-Teaching (CCT). In the RTG phase, descriptions for each sample are generated using a visual lexicon. The CCT phase involves developing a two-stream parametric model that leverages the interaction of visual and textual modalities for enhanced mutual progress. The gray dashed box on the right illustrates the text and image models independently selecting high-confidence samples with pseudo labels for the co-teaching process.

#### 3.2 Baseline

We follow the SimGCD Wen et al. (2023) to build our parametric learning baseline, which consists of a supervised loss for labeled data and an unsupervised loss for both labeled and unlabeled data.

Specifically, the supervised loss utilizes the conventional cross-entropy loss, defined as:

$$\mathcal{L}_{\text{sup}} = \frac{1}{|B^l|} \sum_{i \in B^l} \ell(\mathbf{y}_i, \mathbf{p}_i), \quad (3.1)$$

where  $B^l$  indicates the mini-batch for labeled data,  $\ell$  is the traditional cross-entropy loss, and  $\mathbf{p}_i = \sigma(\mathcal{H}(\mathcal{E}(\mathbf{x}_i))/\tau)$  is the predicted probabilities of input  $\mathbf{x}_i$ . Here,  $\mathcal{E}$  represents the backbone encoder, and  $\mathcal{H}$  indicates the parametric classifier.  $\sigma(\cdot)$  denotes the softmax function, and  $\tau$  is a temperature parameter set to  $\tau_s$ .

For unsupervised loss, we use the predicted probabilities of an augmented counterpart  $\mathbf{x}'_i$  as the supervision to calculate the classification loss for the original input  $\mathbf{x}_i$ , which is formulated as:

$$\mathcal{L}_{\text{unsup}} = \frac{1}{|B|} \sum_{i \in B} \ell(\mathbf{q}'_i, \mathbf{p}_i) - \varepsilon H(\bar{\mathbf{p}}), \quad (3.2)$$

where  $\mathbf{q}'_i$  is the predicted probabilities of  $\mathbf{x}'_i$  using a sharper temperature value  $\tau_t$ . We also include a mean-entropy maximization regularizer  $H(\bar{\mathbf{p}})$  Assran et al. (2022) for the unsupervised objective. Here,  $H(\bar{\mathbf{p}}) = -\sum_k \bar{\mathbf{p}}^{(k)} \log \bar{\mathbf{p}}^{(k)}$ , where  $\bar{\mathbf{p}} = \frac{1}{2|B|} \sum_{i \in B} (\mathbf{p}_i + \mathbf{p}'_i)$ .  $\mathbf{p}_i$  and  $\mathbf{p}'_i$  are the probabilities of  $\mathbf{x}_i$  and  $\mathbf{x}'_i$ , respectively, which use the same temperature of  $\tau_u$ .  $B$  indicates the mini-batch for both labeled and unlabeled data. The hyperparameter  $\varepsilon$  aligns with the configuration used in SimGCD Wen et al. (2023).

The classifier is jointly trained with supervised loss and unsupervised loss, formulated as:

$$\mathcal{L}_{\text{base}} = \lambda \cdot \mathcal{L}_{\text{sup}} + (1 - \lambda) \cdot \mathcal{L}_{\text{unsup}}, \quad (3.3)$$

where  $\lambda$  serves as the balancing factor.

### 3.3 Retrieval-based Text Generation

The existing foundational VLMs and LLMs, trained on massive amounts of data, have demonstrated remarkable capabilities in aligning visual images with corresponding textual descriptions and generating detailed object descriptions. Drawing inspiration from these advancements, we introduce the Retrieval-based Text Generation (RTG) phase for GCD. This process involves two stages: constructing a comprehensive visual lexicon and retrieving probable tags from this lexicon to generate textual information for images.

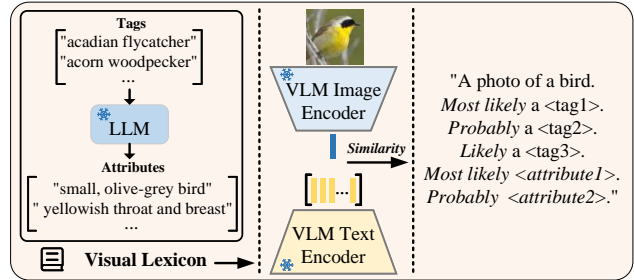


Figure 3: Schema of retrieval-based text generation.

**Building the Visual Lexicon.** To construct a visual lexicon, we aggregate a diverse and extensive collection of tags from established benchmarks in semantic segmentation, object detection and classification. These benchmarks are selected for their comprehensive coverage of the visual categories in the world. Additionally, we utilize a large language model (e.g., GPT3 Brown et al. (2020)) to further describe each tag by using the prompt of “What are useful features for distinguishing a {tag} in a photo?”, which can augment the visual lexicon with the attribute of “{tag} which has the {feature}”.

**Tag Retrieval.** Given the visual lexicon, comprising tags and corresponding attributes, we utilize an auxiliary

VLM (e.g., CLIP Radford et al. (2021)) to encode it, thereby creating a textual feature bank. For each image, we use the auxiliary model to generate its visual feature, which is then compared against the entries in the textual feature bank using cosine similarity. Subsequently, we identify the most relevant  $n_t$  tags and  $n_a$  attributes exhibiting the highest similarity to the image. We then concatenate the textual descriptors of these tags and attributes based on the similarity ranking. This process yields the categorical descriptive text  $\mathbf{t}_i$  for each image  $\mathbf{x}_i$ . The workflow of the RTG phase is delineated in Fig. 3.

**Discussion.** In this paper, we aim to harness the capabilities of the existing foundational models to deliver comprehensive and accurate textual information for GCD. To this end, we employ GPT-3 Brown et al. (2020) as the LLM to obtain attributes and the ViT-H-based CLIP Radford et al. (2021) as the auxiliary VLM to identify tags and attributes. We also attempt to use a smaller auxiliary VLM, e.g., ViT-B-based CLIP, to generate the descriptive text. However, it demonstrated limited efficacy for fine-grained classification because ViT-B-based CLIP tends to focus on more general Tags and Attributes in the Visual Lexicon. Using Flower102 for instance, ViT-B-based CLIP tends to give high similarity to broader Tags like “Plant & Flower”. Compared to existing methods that only use visual cues for GCD, we explore the possibility of introducing the textual information to facilitate the GCD task by using the freely available, public foundational models, which would be a new trend in the community. In addition, our approach enjoys several advantages. Firstly, the RTG is an offline phase, where we only need to process each sample once, avoiding the need for excessive computational overhead. Secondly, given the generated descriptive text, we only need to train the GCD model with a smaller model (ViT-B-based CLIP), achieving significantly higher results than existing methods. Third, the auxiliary VLM can be replaced with other advanced foundational models, such as FLIP Li et al. (2023b) and CoCa Yu et al. (2022). Consequently, the effectiveness of our method is likely to be enhanced in line with the advancements in these foundational models.

### 3.4 Cross-modality Co-teaching

In light of the categorical descriptive texts generated during the RTG phase, the primary challenge lies in effectively utilizing them to train an accurate GCD model. To address this, we develop two-stream parametric classifiers for visual and textual modalities. Recognizing that the intrinsic differences between the modalities naturally meet the requirements for the model disparity in co-teaching strategies Han et al. (2018), we propose a Cross-modal Co-Teaching (CCT) phase to realize the mutual benefits of the visual and textual classifiers. However, a notable challenge arises due to the lack of annotations during the co-teaching process: the classifiers for each modality are often misaligned. This misalignment implies that consistent class indexes across the two modalities cannot be guaranteed, posing a significant obstacle to effective co-teaching. We introduce two preliminary stages to overcome this issue: a warm-up stage and a class-aligning stage, designed to establish modality-specific classifiers while ensuring their alignment.

**Basic Loss.** Given the inputs from two modalities,  $\mathbf{x}_i$  and  $\mathbf{t}_i$ , we construct a text model and an image model based on the parametric baseline in Sec. 3.2. Thus, the basic loss for our method is formulated as:

$$\mathcal{L}_{\text{base}} = \mathcal{L}_{\text{base}}^{\text{I}} + \mathcal{L}_{\text{base}}^{\text{T}}, \quad (3.4)$$

where both components are implemented by Eq. 3.3. The difference is that  $\mathcal{L}_{\text{base}}^{\text{T}}$  is calculated by the text model and textual description.

**Image-Text Contrastive Learning.** To strengthen the association between the image and text modalities, we further introduce a cross-modal contrastive learning between image features and textual features, which is

formulated as:

$$\mathcal{L}_{\text{con}} = \frac{1}{|B|} \sum_{i \in B} -\log \frac{\exp(\mathbf{f}_i^{\text{I}} \cdot (\mathbf{f}_i^{\text{T}})^\top / \tau_c)}{\sum_j \mathbb{I}_{[j \neq i]} \exp(\mathbf{f}_i^{\text{I}} \cdot (\mathbf{f}_j^{\text{T}})^\top / \tau_c)}, \quad (3.5)$$

where  $\tau_c$  is a temperature parameter.  $\mathbf{f}_i^{\text{I}} = \mathcal{E}^{\text{I}}(\mathbf{x}_i)$  is the image feature and  $\mathbf{f}_i^{\text{T}} = \mathcal{E}^{\text{T}}(\mathbf{t}_i)$  is the textual feature.  $\mathcal{E}^{\text{I}}$  and  $\mathcal{E}^{\text{T}}$  represent the image and text encoders, respectively. We next introduce the three stages of the proposed CCT (see Fig. 4), *i.e.*, warm-up, class-aligning, and co-teaching.

**Stage I: Warm-up.** The image and text models initially undergo a warm-up training stage with  $e_w$  epochs, as depicted in Fig 4(a). During this stage, both the text model and image model are trained using the basic loss (Eq. 3.4) and cross-modal contrastive loss (Eq. 3.5). This warm-up training aims to enable both models to adequately learn category knowledge from their respective modality data, thereby developing modality-specific category perceptions.

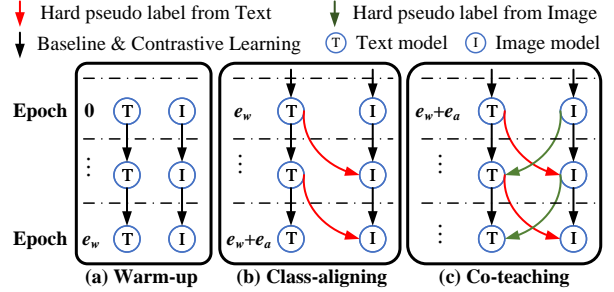


Figure 4: Schema of cross-modality co-teaching.

**Stage II: Class-aligning.** Subsequently, to rectify the class misalignment between image and text classifiers, a class-aligning stage with  $e_a$  epochs is introduced, as illustrated in Fig 4(b). This stage aims to align the classifiers of two modalities. To this end, we select high-confidence samples based on the text model and use them to guide the training of the image model. Specifically, for each category  $k$ , we select the top  $s$  samples that have the highest probabilities in the  $k$ -th category produced by the text model, formulated as  $\text{Top}_k^{\text{T}}(s)$ . In addition, for each sample  $i$  in  $\text{Top}_k^{\text{T}}(s)$ , we assign it with the hard pseudo label of  $\hat{y}_i^{\text{T}} = k$ . Thus, besides the basic and contrastive losses, we additionally train the image model by the pseudo-labeling loss:

$$\mathcal{L}_p^{\text{I}} = \frac{1}{|B^s|} \sum_{i \in B^s} \ell(\hat{y}_i^{\text{T}}, \mathbf{p}_i^{\text{I}}), \quad (3.6)$$

where  $|B^s|$  indicates the number of selected samples in the mini-batch.

**Stage III: Co-teaching.** Following the warm-up and class-aligning stages, we establish cross-modality co-teaching to facilitate the mutual benefit between the image and text models, as shown in Fig 4(c). Similar to the class-aligning stage, we also generate high-confidence samples from the image model, which is defined as  $\text{Top}_k^{\text{I}}(s)$ . For each sample  $i$  in  $\text{Top}_k^{\text{I}}(s)$ , the hard pseudo label is  $\hat{y}_i^{\text{I}} = k$ , and thus the pseudo-labeling loss for the text classifier is formulated as:

$$\mathcal{L}_p^{\text{T}} = \frac{1}{|B^s|} \sum_{i \in B^s} \ell(\hat{y}_i^{\text{I}}, \mathbf{p}_i^{\text{T}}). \quad (3.7)$$

The total loss of Stage III is formulated as:

$$\mathcal{L} = \mathcal{L}_{\text{base}} + \mathcal{L}_{\text{con}} + \mathcal{L}_p^{\text{I}} + \mathcal{L}_p^{\text{T}}. \quad (3.8)$$

**Inference.** When determining the category of object  $i$ , we employ soft voting to merge the category perceptions from both modalities:

$$\mathbf{P}_i = \mathbf{p}_i^{\text{I}} + \mathbf{p}_i^{\text{T}}. \quad (3.9)$$

The predicted category is the one that achieves the largest value in  $P_i$ , *i.e.*,  $\arg \max P_i$ . This integrated approach leverages the strengths of both modalities, leading to more accurate classification.

## 4 Experiments

**Datasets.** We conduct comprehensive experiments on four generic image classification datasets, *i.e.*, CIFAR-10, CIFAR-100 [Krizhevsky et al. \(2009\)](#), ImageNet-100, and ImageNet-1K [Deng et al. \(2009\)](#), as well as on four fine-grained image classification datasets, *i.e.*, CUB [Wah et al. \(2011\)](#), Stanford Cars [Krause et al. \(2013b\)](#), Oxford Pets [Parkhi et al. \(2012\)](#), and Flowers102 [Nilsback & Zisserman \(2008\)](#). Following [Vaze et al. \(2022\)](#), for each dataset, we select half of the classes as the known classes and the remaining as the unseen classes. We select 50% of samples from the known classes as the labeled dataset  $\mathcal{D}_L$  and regard the remaining samples as unlabeled dataset  $\mathcal{D}_U$  that are from both known and unseen classes. Refer to the Appendix 6 material for details about the datasets.

**Evaluation Protocol.** Following [Vaze et al. \(2022\)](#), we use the clustering accuracy (ACC) to evaluate the performance of each algorithm. Specifically, the ACC is calculated on the unlabeled data, formulated as  $ACC = \frac{1}{|\mathcal{D}_U|} \sum_{i=1}^{|\mathcal{D}_U|} \mathbb{I}(y_i = C(\bar{y}_i))$ , where  $\bar{y} = \arg \max \mathbf{P}$  represents the predicted labels and  $y$  denotes the ground truth. The  $C$  denotes the optimal permutation, aligning predicted cluster assignments with the actual class labels.

**Implementation Details.** We construct the tag lexicon by incorporating tags from semantic segmentation and object detection datasets [Gupta et al. \(2019\)](#); [Lin et al. \(2014\)](#); [Kuznetsova et al. \(2020\)](#), image classification datasets [Russakovsky et al. \(2015\)](#); [Li et al. \(2022a\)](#); [Cimpoi et al. \(2014\)](#); [Parkhi et al. \(2012\)](#); [Bossard et al. \(2014\)](#); [Xiao et al. \(2010\)](#); [Krause et al. \(2013a\)](#) and visual genome dataset [Krishna et al. \(2017\)](#). The CLIP [Radford et al. \(2021\)](#) model with a ViT-B-16 architecture serves as the backbone, ensuring a fair comparison to methods utilizing the DINO [Caron et al. \(2021\)](#) model with the same architecture. A linear classifier layer is added after the backbone for each modality. During training, only the last layers of both the text and image encoders in the backbone are fine-tuned, using a learning rate of 0.0005. The learning rates for classifiers start at 0.1 and decrease following a cosine annealing schedule. We train the model for 200 epochs on all datasets, using a batch size of 128 and processing dual views of randomly augmented images and texts. The temperature parameters  $\tau_s$  and  $\tau_u$  are set at 0.1 and 0.05, respectively.  $\tau_t$  starts at 0.035 and decreases to 0.02, except for CIFAR-10 where it varies from 0.07 to 0.04 due to fewer classes. We use the logit scale value to set  $\tau_c$  as in the CLIP model. The balancing factor  $\lambda$  is set to 0.2. Warm-up and class-aligning stages last for 10 and 5 epochs, respectively, denoted as  $e_w = 10$  and  $e_a = 5$ . For selecting high-confidence samples, we choose  $s = r * \frac{|\mathcal{D}_U|}{K}$  samples per category, with  $r$  set at 0.6. In line with SimGCD [Wen et al. \(2023\)](#), we conduct each experiment three times, and the average result over the three runs is reported.

### 4.1 Comparison with the State of the Art

We conduct a comparative analysis between our proposed TextGCD and leading methods in GCD, as delineated in Tab. 1 and Tab. 2. These methods encompass GCD [Vaze et al. \(2022\)](#), SimGCD [Wen et al. \(2023\)](#), DCCL [Pu et al. \(2023\)](#), GPC [Zhao et al. \(2023\)](#), PromptCAL [Zhang et al. \(2023\)](#), CLIP-GCD [Ouldoughi et al. \(2023\)](#) and SPTNet [Wang et al. \(2023\)](#). Except for CLIP-GCD [Ouldoughi et al. \(2023\)](#), which uses CLIP as the backbone, the others utilize the DINO as the backbone. To better ensure the fairness of our comparison, we also reproduce SimGCD by using CLIP as the backbone. Clearly, our TextGCD outperforms



all compared methods in terms of All accuracy on all datasets. Importantly, compared to the best competitor, SimGCD, our method achieves a significant improvement on the challenging ImageNet-1K and all the fine-grained datasets. Specifically, our method outperforms SimGCD by 7.7% in All accuracy and 11.4% in New accuracy on the ImageNet-1K dataset, and, by 11.1% in All accuracy and 12.7% in New accuracy averaged on fine-grained datasets. This demonstrates the superiority of our method over existing visual-based methods. In comparison to CLIP-GCD, which merely concatenates features from both modalities, TextGCD achieves higher results. For instance, TextGCD surpasses CLIP-GCD by 13.8%, 16.3%, and 10.9% in terms of All accuracy on the CUB, Stanford Cars, and Flowers102 datasets, respectively.

Table 1: Results on generic datasets. The best results are highlighted in **bold**.

Methods	Backbone	CIFAR-10			CIFAR-100			ImageNet-100			ImageNet-1K		
		All	Old	New	All	Old	New	All	Old	New	All	Old	New
GCD Vaze et al. (2022)	DINO	91.5	97.9	88.2	73.0	76.2	66.5	74.1	89.8	66.3	52.5	72.5	42.2
SimGCD Wen et al. (2023)	DINO	97.1	95.1	98.1	80.1	81.2	77.8	83.0	93.1	77.9	57.1	77.3	46.9
DCCL Pu et al. (2023)	DINO	96.3	96.5	96.9	75.3	76.8	70.2	80.5	90.5	76.2	-	-	-
GPC Zhao et al. (2023)	DINO	92.2	<b>98.2</b>	89.1	77.9	85.0	63.0	76.9	94.3	71.0	-	-	-
PromptCAL Zhang et al. (2023)	DINO	97.9	96.6	98.5	81.2	84.2	75.3	83.1	92.7	78.3	-	-	-
SPTNet Wang et al. (2023)	DINO	97.3	95.0	<b>98.6</b>	81.3	84.3	75.6	85.4	93.2	81.4	-	-	-
CLIP-GCD Ouldoughi et al. (2023)	CLIP	96.6	97.2	96.4	85.2	85.0	<b>85.6</b>	84.0	<b>95.5</b>	78.2	-	-	-
SimGCD Wen et al. (2023)	CLIP	96.6	94.7	97.5	81.6	82.6	79.5	86.1	94.5	81.9	48.2	72.7	36.0
TextGCD	CLIP	<b>98.2</b>	98.0	<b>98.6</b>	<b>85.7</b>	<b>86.3</b>	84.6	<b>88.0</b>	92.4	<b>85.2</b>	<b>64.8</b>	<b>77.8</b>	<b>58.3</b>

Table 2: Results on fine-grained datasets. The best results are highlighted in **bold**.

Methods	Backbone	CUB			Stanford Cars			Oxford Pets			Flowers102		
		All	Old	New	All	Old	New	All	Old	New	All	Old	New
GCD Vaze et al. (2022)	DINO	51.3	56.6	48.7	39.0	57.6	29.9	80.2	85.1	77.6	74.4	74.9	74.1
SimGCD Wen et al. (2023)	DINO	60.3	65.6	57.7	53.8	71.9	45.0	87.7	85.9	88.6	71.3	80.9	66.5
DCCL Pu et al. (2023)	DINO	63.5	60.8	64.9	43.1	55.7	36.2	88.1	88.2	88.0	-	-	-
SPTNet Wang et al. (2023)	DINO	65.8	68.8	65.1	59.0	79.2	49.3	-	-	-	-	-	-
CLIP-GCD Ouldoughi et al. (2023)	CLIP	62.8	77.1	55.7	70.6	<b>88.2</b>	62.2	-	-	-	76.3	88.6	70.2
SimGCD Wen et al. (2023)	CLIP	62.0	76.8	54.6	75.9	81.4	73.1	88.6	75.2	95.7	75.3	87.8	69.0
TextGCD	CLIP	<b>76.6</b>	<b>80.6</b>	<b>74.7</b>	<b>86.9</b>	87.4	<b>86.7</b>	<b>95.5</b>	<b>93.9</b>	<b>96.4</b>	<b>87.2</b>	<b>90.7</b>	<b>85.4</b>

## 4.2 Ablation Study

**Components Ablation.** In Tab. 3, we present an ablation study of the key components in TextGCD, specifically cross-modality co-teaching, contrastive learning, and soft voting. Beginning with the Baseline method, we incrementally incorporate these three components into the framework to evaluate their impact on the performance of both image and text classifiers. We also report the results of 1) employing the first tag derived from the visual lexicon as the GCD labels and 2) performing  $k$ -means MacQueen et al. (1967) using the image or text features without training. It becomes evident that the “First-Tag” and “ $k$ -means” methods yield inferior results compared to the baseline. On the other hand, the “ $k$ -means” method and the baseline results demonstrate that using the textual information achieves clearly higher results than using the image cues, thereby highlighting the superior quality of the generated textual descriptions. Compared to the baseline, integrating our proposed co-teaching approach markedly elevates the performance across both modalities, particularly notable within the context of the fine-grained CUB dataset. This substantiates the efficacy of our co-teaching strategy in fostering synergistic learning and collaborative advancement between text and image models. Furthermore, image-text contrastive learning consistently increases the All and New

Table 3: Ablation study on TextGCD components. “T” and “I” denote the output results of the text and image classifiers, respectively. “First-Tag” refers to the accuracy achieved using the most similar tag from the visual lexicon as the label. “ $k$ -means” indicates applying  $k$ -means on the initial backbone features.

Methods	Classifier	CIFAR-100			CUB		
		All	Old	New	All	Old	New
First-Tag	-	12.0	12.0	11.9	47.8	43.4	52.1
$k$ -means	T	70.2	66.6	77.5	67.6	64.5	69.2
	I	46.5	45.6	48.5	46.7	50.6	44.7
Baseline	T	81.8	83.6	78.3	67.0	75.9	62.6
	I	76.3	80.9	67.0	49.0	64.2	41.3
+Co-Teaching	T	84.4	86.2	81.1	74.4	79.3	72.0
	I	82.4	85.0	77.3	71.7	79.4	67.8
+Contrastive	T	84.6	84.8	84.1	74.8	78.6	73.0
	I	83.1	84.0	81.1	73.9	80.4	70.7
+Soft Voting	-	<b>85.7</b>	<b>86.3</b>	<b>84.6</b>	<b>76.6</b>	<b>80.6</b>	<b>74.7</b>

accuracies, underlining the necessity of aligning the two modalities. Ultimately, soft voting can further improve performance, illustrating that the integration of information from both modalities leads to more precise category discrimination.

**Training Stages Ablation.** In Tab. 4, we assess the impact of each stage within the proposed CCT phase, *i.e.*, warm-up, class-aligning, and co-teaching. Results show that using co-teaching solely achieves lower results than our full method. Specifically, the warm-up process is important for the fine-grained dataset, *i.e.*, CUB and SCars. On the other hand, the class-aligning consistently improves the performance on all four datasets, which obtains 10.5%, 9.2%, 0.6%, and 2.7% in New accuracy on CIFAR-100, ImageNet-100, CUB and SCars, respectively. This observation highlights the vital role of class-aligning stage in resolving conflicts between the two classifiers. To further investigate the proposed class-aligning strategy, we evaluate the variant of using the image model to guide the text model, denoted as “I→T”. In terms of All and New accuracies, we observe that 1) both strategies can achieve consistent improvements (except for “I→T” on CUB) and that 2) the proposed text-guide-image strategy produces higher results than the image-guide-text variant in most cases. These advantages can be attributed to the more representative initial features generated by the textual descriptions. Therefore, the discriminative textual features can generate high-quality pseudo-labels for effectively guiding visual model (text-guide-image) or can be robust to noisy labels when guided by the visual model (image-guide-text). This further demonstrates the importance of introducing textual modality into our co-teaching framework.

Table 4: Ablation study on TextGCD training stages. “Warm-up” refers to the warm-up stage and “Cls. Align” denotes the class-aligning stage. “T→I” signifies aligning the image model using the text model, whereas “I→T” indicates aligning the text model using the image model.

Warm-up	Cls. Align		Co-Teaching	CIFAR-100			ImageNet-100			CUB			Stanford Cars		
	I→T	T→I		All	Old	New	All	Old	New	All	Old	New	All	Old	New
			✓	83.3	86.8	76.4	80.6	92.8	74.5	74.8	77.4	73.5	83.9	88.1	80.6
✓			✓	82.8	<b>87.2</b>	74.1	81.6	92.6	76.0	76.5	<b>81.2</b>	74.1	85.3	<b>87.8</b>	84.0
✓	✓		✓	84.6	86.6	80.6	87.5	<b>93.5</b>	84.4	76.1	80.9	73.6	<b>87.5</b>	86.4	<b>87.9</b>
✓		✓	✓	<b>85.7</b>	86.3	<b>84.6</b>	<b>88.0</b>	92.4	<b>85.2</b>	<b>76.6</b>	80.6	<b>74.7</b>	86.9	87.4	86.7

### 4.3 Evaluation

**Backbone Evaluation.** In Tab. 5, we evaluate the impact of the image encoder in TextGCD by substituting the image encoder of CLIP with that of DINO, while maintaining the text encoder from CLIP. In TextGCD(DINO), we omit the cross-modal contrastive loss  $\mathcal{L}_{\text{con}}$ . Despite a decreased accuracy on CUB, TextGCD(DINO) still significantly outperforms SimGCD, which utilizes the same image encoder.

Table 5: Evaluation on different pretrained ViT-B backbones.

Methods	Backbone	CIFAR-100			CUB		
		All	Old	New	All	Old	New
SimGCD	DINO	80.1	81.2	77.8	60.3	65.6	57.7
TextGCD	DINO	<b>86.1</b>	<b>88.7</b>	81.0	73.7	80.3	70.4
TextGCD	CLIP	85.7	86.3	<b>84.6</b>	<b>76.6</b>	<b>80.6</b>	<b>74.7</b>

Moreover, we compare SimGCD and TextGCD using the ViT-H-based CLIP for a more fair comparison, as we use the ViT-H for text generation. Tab. 6 shows that our TextGCD outperforms SimGCD by a large margin on both datasets. Interestingly, both SimGCD and our method show a decrease in performance on the generic dataset CIFAR-100, in terms of New accuracy, compared to the ones using ViT-B-16 as the backbone (see Tab. 1). This suggests that fine-tuning on the generic dataset may adversely affect the ability of the large model. In addition, we can observe a small margin between our methods with ViT-B-16 and ViT-H-14. This indicates that our advantage mainly benefited from the high-quality text description and the co-teaching strategy, enabling our approach to adapt to both smaller and larger models.

Table 6: Evaluation on ViT-H-14 backbone.

Methods	CLIP Backbone	CIFAR-100			CUB		
		All	Old	New	All	Old	New
SimGCD	ViT-H-14	78.1	80.0	74.4	69.1	76.3	65.4
TextGCD	ViT-H-14	<b>86.4</b>	<b>89.3</b>	<b>80.7</b>	<b>78.6</b>	<b>81.5</b>	<b>77.1</b>

**Text Generation Evaluation.** In Tab. 7, we analyze the impact of the number of tags and attributes for constructing category descriptions in the RTG phase. Results show that richer textual content (more tags and attributes) leads to higher category recognition accuracy. Due to the token limitation of CLIP, we can use up to only three tags and two attributes in the input of the text model. We will handle this drawback and investigate the impact of including more tags and attributes in future work.

Table 7: Evaluation on the number of tags and attributes.

# Tag	# Attribute	CIFAR-100			CUB		
		All	Old	New	All	Old	New
1	0	81.6	81.6	81.8	67.9	69.6	67.0
2	0	83.5	83.4	83.7	68.6	75.3	65.3
3	0	83.7	84.7	81.6	69.9	74.9	67.3
3	1	84.7	85.4	83.4	74.7	80.5	71.7
3	2	<b>85.7</b>	<b>86.3</b>	<b>84.6</b>	<b>76.6</b>	<b>80.6</b>	<b>74.7</b>

**Auxiliary Model Evaluation.** In Tab. 8, we explore the effect of substituting the auxiliary model with

FLIP Li et al. (2023b) and CoCa Yu et al. (2022). Results show that our method consistently produces high performance on both datasets and that using a more powerful model (FLIP) leads to higher results.

Table 8: Evaluation on the auxiliary model.

Auxiliary Model	Backbone	CIFAR-100			CUB		
		All	Old	New	All	Old	New
CLIP Radford et al. (2021)	ViT-H-14	85.7	86.3	84.6	76.6	80.6	74.7
CoCa Yu et al. (2022)	ViT-L-14	85.2	85.8	83.8	73.6	81.7	69.5
FLIP Li et al. (2023b)	ViT-G-14	<b>87.6</b>	<b>87.7</b>	<b>87.5</b>	<b>79.5</b>	<b>83.5</b>	<b>77.4</b>

**Co-Teaching Strategy Evaluation.** To demonstrate the effectiveness of the cross-modal co-teaching strategy, we conduct a comparative analysis with a co-teaching approach utilizing a single modality. Results in Tab. 9 show that single-modality co-teaching variants obtain lower results than the proposed cross-modality co-teaching. This finding highlights the critical role of ensuring the model diversity in co-teaching.

Table 9: Evaluation on co-teaching strategies. “I↔T” is our cross-modality co-teaching. “T↔T” and “I↔I” indicate the single-modality variant using text modality and image modality, respectively.

Methods	CIFAR-100			CUB		
	All	Old	New	All	Old	New
T↔T	79.8	83.6	72.1	71.7	73.0	71.1
I↔I	75.5	80.5	65.7	60.3	79.5	50.7
I↔T (Ours)	<b>85.7</b>	<b>86.3</b>	<b>84.6</b>	<b>76.6</b>	<b>80.6</b>	<b>74.7</b>

#### 4.4 Hyper-parameters Analysis

**Balancing Factor  $\lambda$  and Proportion Coefficient  $r$ .** The impact of the balancing factor  $\lambda$  and the proportion coefficient  $r$  is illustrated in Fig. 5. We use All accuracy as the evaluation metric. An increase in  $\lambda$  suggests that the classifiers of both models increasingly prioritize labeled data from known categories. Results show that  $\lambda = 0.2$  achieves the best accuracy on both datasets. The parameter  $r$  determines the fraction of high-confidence samples chosen from each category for the text and image models. A higher value of  $r$  is typically advantageous, and the best result is achieved when  $r = 0.6$ . Note that we use the same hyper-parameters ( $\lambda$  and  $r$ ) for all datasets to avoid over-tuning.

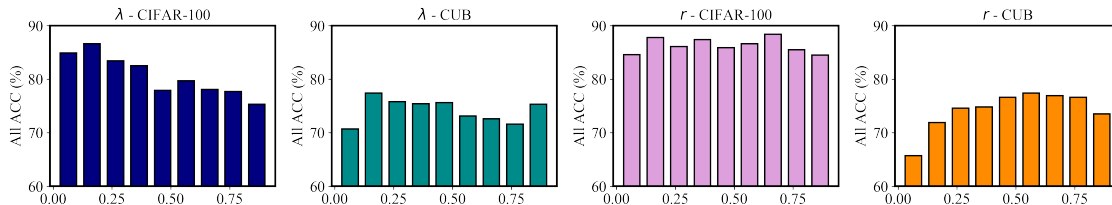


Figure 5: Impact of hyper-parameters.

## 5 Limitations

**Dependency on the Visual Lexicon.** The effectiveness of our method largely depends on a rich visual lexicon. Although massive category names have been gathered from existing datasets, it might still lack the categories in specific tasks, such as the Herbarium 19 dataset [Tan et al. \(2019\)](#) designed for botanical research. In such a context, our method may fail to produce informative textual descriptions and thus produce inferior results.

**Inheriting Flaws from Foundation Models.** Owing to our reliance on LLMs and VLMs for constructing category descriptive texts, our method inevitably inherits biases and drawbacks from these foundational models. For example, as shown in Tab. 10, the CLIP model exhibits suboptimal performance (Zero-Shot) on the FGVC Aircraft dataset [Maji et al. \(2013\)](#). As a result, our method fails to generate informative text descriptions and cannot obtain improvement compared to the visual-only competitor SimGCD.

Table 10: Comparison on the FGVC Aircraft dataset. “Zero Shot” indicates building the textual classifier with ground-truth names and directly performing classification.

Methods	All	Old	New
Zero Shot	15.9	10.8	20.9
GCD	45.0	41.1	46.9
SimGCD	<b>54.2</b>	<b>59.1</b>	51.8
Ours	50.8	44.9	<b>53.8</b>

## 6 Conclusion

In this paper, we introduce a novel approach called TextGCD for Generalized Category Discovery. Compared to previous methods that only rely on visual patterns, we additionally integrate textual information into the framework. Specifically, we first construct a visual lexicon based on off-the-shelf category tags and enrich it with attributes by Large Language Models (LLMs). Following this, a Retrieval-based Text Generation (RTG) approach is proposed to assign each sample with likely tags and corresponding attributes. Building upon this, we design a Cross-modal Co-Teaching (CCT) strategy to fully take the mutual benefit between visual and textual information, enabling robust and complementary model training. Experiments on eight benchmarks show that our TextGCD produces new state-of-the-art performance. We hope this study could bring a new perspective, which assists the framework with foundational model and textual information, for the GCD community.

## Appendix

### A. Datasets Settings

In the main paper, we follow the GCD protocol [Vaze et al. \(2022\)](#) to determine the number of known classes in the dataset and the number of labeled data samples selected from these classes. As illustrated in Fig. 6, the blue segment denotes the labeled data, whereas the yellow segment encompasses the unlabeled data, which includes both known and unknown categories. We conduct extensive experiments across four generic image classification datasets, namely, CIFAR-10, CIFAR-100 [Krizhevsky et al. \(2009\)](#), ImageNet-100, and

ImageNet-1K [Deng et al. \(2009\)](#), and four fine-grained image classification datasets, specifically, CUB [Wah et al. \(2011\)](#), Stanford Cars [Krause et al. \(2013b\)](#), Oxford Pets [Parkhi et al. \(2012\)](#), and Flowers102 [Nilsback & Zisserman \(2008\)](#). Detailed dataset information is provided in Table 11.

Table 11: Statistics of the datasets for GCD.

Dataset	Labelled		Unlabelled	
	#Image	#Class	#Image	#Class
ImageNet-100 <a href="#">Deng et al. (2009)</a>	31.9K	50	95.3K	100
ImageNet-1K <a href="#">Deng et al. (2009)</a>	321K	500	960K	1000
CIFAR-10 <a href="#">Krizhevsky et al. (2009)</a>	12.5K	5	37.5K	10
CIFAR-100 <a href="#">Krizhevsky et al. (2009)</a>	20.0K	80	30.0K	100
CUB <a href="#">Wah et al. (2011)</a>	1.5K	100	4.5K	200
Stanford Cars <a href="#">Krause et al. (2013b)</a>	2.0K	98	6.1K	196
Oxford Pets <a href="#">Parkhi et al. (2012)</a>	0.9K	19	2.7K	37
Flowers102 <a href="#">Nilsback &amp; Zisserman (2008)</a>	0.3K	51	0.8K	102

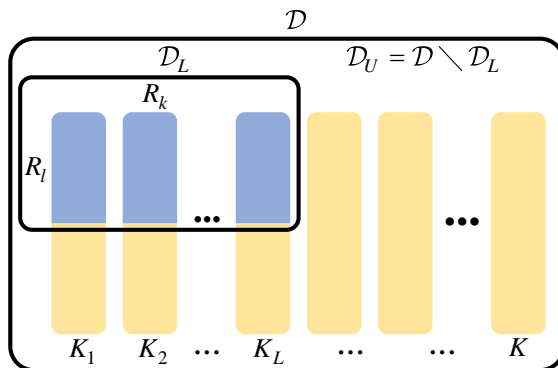


Figure 6: Configuration of the Dataset for the GCD Task.

## B. Extended Experiment Results

### B.1. Main Results

**Mean & Std.** In the main paper, we present the full results as the average of three runs to mitigate the impact of randomness. Detailed outcomes for TextGCD, encompassing mean values and population standard deviation, are delineated in Tab. 12.

Table 12: Mean and Std of Accuracy in Three Independent Runs

Dataset	All	Old	New
CIFAR10 <a href="#">Krizhevsky et al. (2009)</a>	98.2±0.3	98.0±0.1	98.6±0.5
CIFAR100 <a href="#">Krizhevsky et al. (2009)</a>	85.7±0.6	86.3±0.6	84.6±0.9
ImageNet-100 <a href="#">Deng et al. (2009)</a>	88.0±0.7	92.4±0.3	85.2±1.2
ImageNet-1K <a href="#">Deng et al. (2009)</a>	64.8±0.1	77.8±0.1	58.3±0.1
CUB <a href="#">Wah et al. (2011)</a>	76.6±1.0	80.6±0.8	74.7±1.1
Stanford Cars <a href="#">Krause et al. (2013b)</a>	86.9±0.6	87.4±1.0	86.7±0.4
Oxford Pets <a href="#">Parkhi et al. (2012)</a>	95.5±0.1	93.9±0.6	96.4±0.1
Flowers102 <a href="#">Nilsback &amp; Zisserman (2008)</a>	87.2±1.7	90.7±0.9	85.4±2.5

**Results Through Training.** We employ the CUB dataset as a case study to illustrate the model’s predictive

performance evolution during training, depicted as a curve across epochs. This representation includes results from the text model, the image model, and the soft voting mechanism, as indicated in Fig. 7. The graph reveals two key observations: 1) Implementing the class-aligning stage (commencing at the  $e_w$ -th epoch) and the co-teaching stage (initiating at the  $e_w+e_a$ -th epoch) markedly improves the identification of previously unseen categories. 2) Integrating insights from different modalities via soft voting enhances the overall prediction accuracy.

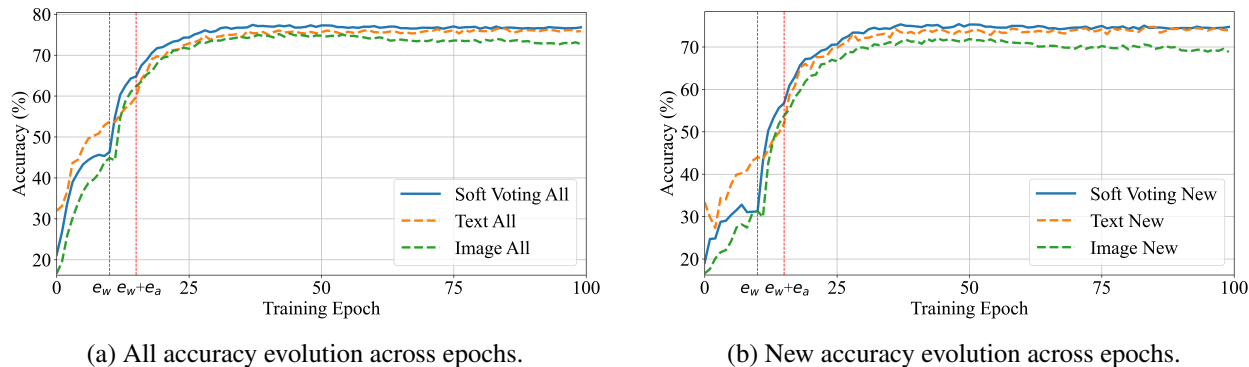


Figure 7: Training accuracy over epochs on the CUB dataset.

## B.2. Evaluation on Varying Known Knowledge

In the main paper, we adhere to the GCD protocol Vaze et al. (2022) for setting the number of known classes in the dataset and the number of labeled data samples selected from these classes. The number of selected known categories is denoted as  $K_L = R_k * K$ . The variable  $R_l$  represents the proportion of data labeled from each known category. Therefore,  $R_k$  and  $R_l$  together determine the amount of labeled data. Following Vaze et al. (2022), we set  $R_k$  to 0.5 for most datasets, except for CIFAR-100, where  $R_k$  is set to 0.8.  $R_l$  is maintained at 0.5 across all datasets. We compare SimGCD Wen et al. (2023) with our TextGCD on the CIFAR-100 and CUB datasets to assess the influence of hyper-parameters  $R_k$  and  $R_l$ . To minimize the effects of randomness, each experiment is conducted three times, and the average All accuracy is reported.

Lower values of  $R_k$  and  $R_l$  correspond to reduced prior knowledge, thereby elevating the difficulty level of the GCD task. As shown in Fig. 8, in scenarios characterized by limited prior knowledge, our TextGCD method demonstrates a notable advantage over SimGCD. Notably, when merely 10% of data from each known category is designated as labeled data, TextGCD exhibits an improvement of 31.2% over SimGCD. This exceptional performance can be attributed to two main reasons: firstly, the introduction of the textual modality brings additional prior knowledge; secondly, the accurate prior knowledge of the textual modality is obtained during the RTG phase.

## B.3. Evaluation on Pseudo Label Forms

In Tab. 13, we evaluate the effectiveness of different pseudo-labeling approaches in the co-teaching process. Our results demonstrate that the use of hard pseudo labels significantly surpasses soft pseudo labels, with an average improvement of 6.8% in All accuracy across both datasets. This finding suggests that hard pseudo labels are more advantageous for the co-teaching process.

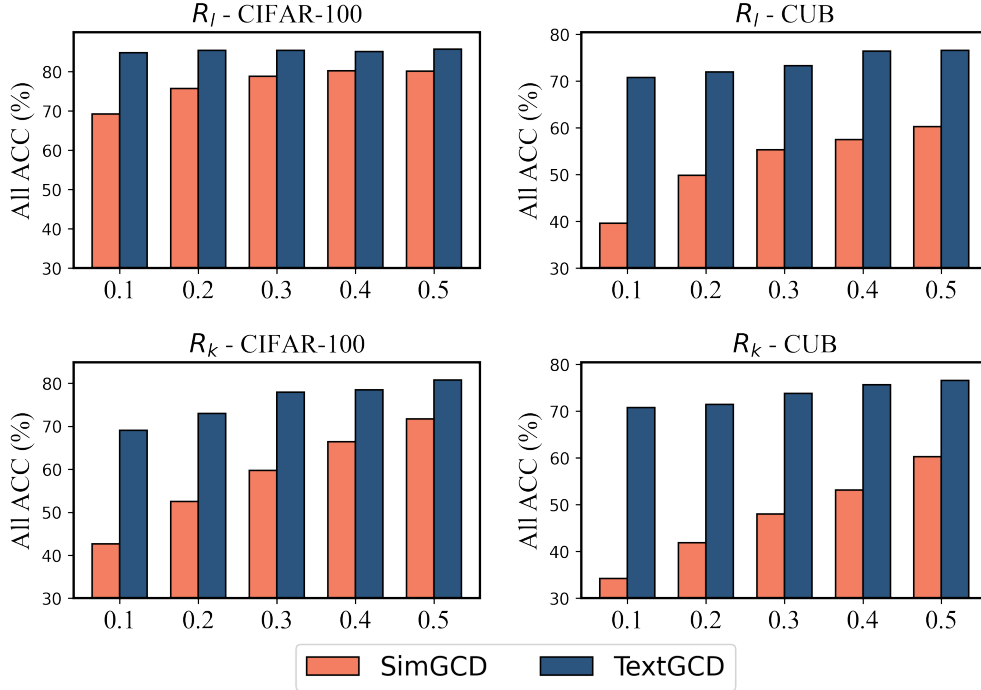


Figure 8: Comparative analysis of TextGCD and SimGCD with varying hyper-parameters  $R_k$  and  $R_l$ .

Table 13: Evaluation on pseudo label forms. “Soft” denotes the use of predicted probabilities from each model (image and text) as pseudo labels for the other, while “Hard” indicates the application of hard pseudo labels in co-teaching.

Methods	CIFAR 100			CUB		
	All	Old	New	All	Old	New
Soft	77.6	79.3	74.1	72.9	77.2	70.8
Hard	<b>85.7</b>	<b>86.3</b>	<b>84.6</b>	<b>76.6</b>	<b>80.6</b>	<b>74.7</b>

#### B.4. Generating Text for Images Using BLIP

BLIP Li et al. (2022b) introduces an optimization objective for generative tasks, facilitating the generation of textual descriptions for images. We explore using BLIP Li et al. (2022b) (blip-large) and BLIP2 Li et al. (2023a) (blip2-opt-2.7b) to generate textual content for images. For equitable comparison, we employ prompts such as “The name of this object/bird is” for tag generation and “The feature of this object/bird is” for attribute generation. These elements—three tags and two attributes—are then amalgamated to construct descriptive texts for images. As demonstrated in Tab. 14, although using BLIP2 for text generation shows some improvement on the general dataset CIFAR-100, the methods employing BLIP and BLIP2 yield results significantly inferior to our retrieval-based method on the fine-grained dataset CUB. In particular, our method surpasses the BLIP2-based method by 35.7% in All accuracy. This underperformance is attributed to BLIP’s tendency to overlook detailed content, thus limiting its accuracy in fine-grained class discovery.



Table 14: Comparative analysis of text generation using BLIP.

Methods	CIFAR 100			CUB		
	All	Old	New	All	Old	New
BLIP-based	74.1	75.6	71.0	36.2	48.7	29.9
BLIP2-based	<b>87.8</b>	<b>87.9</b>	<b>87.5</b>	40.9	59.3	31.6
Retrieval-based (Ours)	85.7	86.3	84.6	<b>76.6</b>	<b>80.6</b>	<b>74.7</b>

## B.5. Visualization of Feature Distributions

To further evaluate the effectiveness of TextGCD, we utilize t-SNE for visualizing feature representations generated by the backbone network. We compare the trained backbones of GCD, SimGCD, and our TextGCD on the Oxford Pets [Parkhi et al. \(2012\)](#) dataset. As depicted in Fig. 9 (a), (b), and (c)—all utilizing ViT-B as the backbone—it is evident that TextGCD produces more discriminative feature representations. Moreover, Fig. 9 (d) further validates the effectiveness of TextGCD’s textual feature representations.

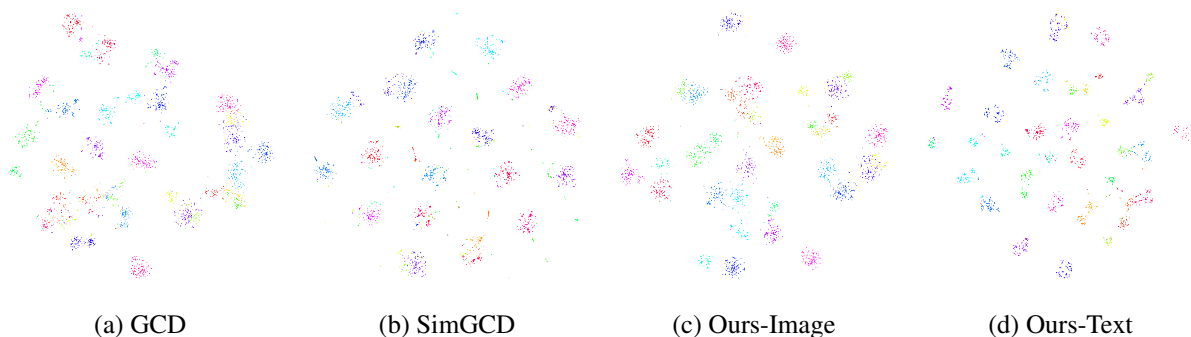


Figure 9: Visualization of feature distributions of the unlabeled set of the Oxford Pets dataset.

## C. Discussion and Future Direction

**Visual Lexicon Selection.** There is overlap between the datasets used for evaluation and those used to build the Visual Lexicon. Specifically, ImageNet-1K is utilized in both contexts. Our goal is to collect as much object semantics as possible to construct a rich and diverse Visual Lexicon. Given its popularity and the extensive common visual object semantics it contains, which are also prevalent in other datasets, ImageNet-1K’s class names are included when constructing the Visual Lexicon.

**Tailored Visual Lexicon.** Since labeled data are available in the GCD task, they can be used to confirm the scope of classified images, especially for fine-grained classification. We create a tailored Visual Lexicon for the Flower102 dataset by employing an LLM (Llama-2-13b) model to filter out tags unrelated to flowers and plants. As shown in Tab. 15, the tailored Visual Lexicon leads to improved results. In our future work, we plan to construct unique Visual Lexicons for each dataset.

Table 15: Evaluation about Visual Lexicon on Flower102.

Methods	All	Old	New
Original Lexicon	87.2	90.7	85.4
Tailored Lexicon	<b>88.3</b>	<b>91.4</b>	<b>86.8</b>

## D. Illustration

### D.1. Visual Lexicon

During the RTG phase, we introduce the category understanding capabilities of LLMs (GPT-3) to expand the Visual Lexicon. According to Tab.7 in the main paper, the introduction of attributes has led to improvements across both generic datasets and fine-grained classification datasets. Some examples from the Visual Lexicon are presented in Tab. 16.

Table 16: Examples in the Visual Lexicon.




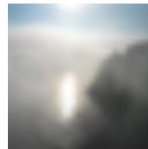
<b>Abyssinian cat</b> <ul style="list-style-type: none"><li>• which has medium-sized cat</li><li>• which has short, soft coat</li><li>• which has distinctive ticked tabby pattern</li><li>• which has large pointed ears</li><li>• which is almond-shaped eyes</li><li>• which has long, lean body</li></ul>
<b>Bengal cat</b> <ul style="list-style-type: none"><li>• which has medium-sized cat with a muscular body</li><li>• which has thick fur in various shades of brown and black</li><li>• which has faint horizontal stripes on the neck, face, and legs</li><li>• which has large, round eyes in shades of gold and green</li><li>• which has pointed ears</li></ul>
<b>Birman cat</b> <ul style="list-style-type: none"><li>• which has medium-sized cat</li><li>• which has long, flowing coat</li><li>• which has white feet</li><li>• which has sapphire blue eyes</li><li>• which has white muzzle</li><li>• which has medium-length tail</li><li>• which has long, silky fur</li></ul>
<b>Bombay cat</b> <ul style="list-style-type: none"><li>• which has short, dense coat</li><li>• which has black or black-brown coat with copper highlights</li><li>• which has large, rounded ears</li><li>• which is a broad chest and muscular body</li><li>• which is a short, thick tail</li><li>• which has four white paws and a white chin</li></ul>
<b>British Shorthair cat</b> <ul style="list-style-type: none"><li>• which has short-haired, stocky cat</li><li>• which has large, round eyes</li><li>• which has broad head and cheeks</li><li>• which has short, dense fur</li><li>• which has short, thick legs</li><li>• which has short, thick tail</li></ul>

### D.2. Categorical Descriptive Text

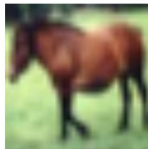

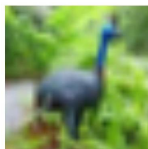

In Fig. 10 and Fig. 11, we showcase examples of descriptive text generated during the RTG phase. For images with distinct features, the generated text accurately describes the categories, as illustrated in Fig. 10 (a.1 2), Fig. 10 (c.1,2,3), and Fig. 11 (a.1,2; b.1,2). In some cases, the descriptive text displays categories closely related to the ground truth, such as “monorail” and “maglev” for “Train” in Fig. 10 (a.3), and “trailer truck” and “commercial vehicle” for “Truck” in Fig. 10 (b.2). Additionally, the text sometimes presents subcategories of the ground truth, like “Peafowl” and “Cassowary” for “Bird” in Fig. 10 (b.3). This textual information aids in achieving precise category differentiation, facilitating mutual enhancement with visual modalities during the co-teaching phase.

However, there are instances where the text generates incorrect category descriptions, such as in Fig. 10 (a.4), (b.4), (c.4) and Fig. 11 (a.4), (c.4), (d.4). Yet, these category descriptive texts reflect certain features of the true categories. For example, “fog” and “sky” in Fig. 10 (a.4) are relevant to “Cloud”; “Pronghorn”, “Mountain





goat”, and “deer” share similar appearances in Fig. 10 (b.4); “Peruvian lily”, “daylily”, and “dwarf day lily” in Fig. 11 (a.4) belong to the lily family. On one hand, this association promotes mutual learning during the co-teaching process. On the other hand, we utilize a soft voting mechanism to combine the category determinations from textual and visual modalities, jointly deciding on category divisions. This approach helps to reduce misjudgments made by relying on a single modality.

Images	Selected Tags & Attributes	Images	Selected Tags & Attributes
	<i>Most likely a african elephant;</i> <i>Probably a elephant;</i> <i>Likely a asian elephant;</i> <i>Most likely elephant which has large mammal;</i> <i>Probably adult, elephant which has large, fourlimbed mammal.</i>		<i>Most likely a typing;</i> <i>Probably a computer keyboard;</i> <i>Likely a email;</i> <i>Most likely computer keyboard which is a spacebar;</i> <i>Probably computer keyboard which is a mouse or trackpad.</i>
(1) Ground-truth: Elephant		(2) Ground-truth: Keyboard	
	<i>Most likely a monorail;</i> <i>Probably a personal rapid transit;</i> <i>Likely a maglev;</i> <i>Most likely bullettrain which has long, narrow body;</i> <i>Probably Bullettrain which is aerodynamic body.</i>		<i>Most likely a crater lake;</i> <i>Probably a piton;</i> <i>Likely a paragliding;</i> <i>Most likely glare which has haze or fog in the image;</i> <i>Probably haze which is a hazy sky with low visibility.</i>
(3) Ground-truth: Train		(4) Ground-truth: Cloud	

(a) Examples in CIFAR-100

Images	Selected Tags & Attributes	Images	Selected Tags & Attributes
	<i>Most likely a horse;</i> <i>Probably a Mustang horse;</i> <i>Likely a Shetland pony;</i> <i>Most likely common sorrel horse which has reddishbrown coat;</i> <i>Probably common sorrel horse which has short ears.</i>		<i>Most likely a trailertruck;</i> <i>Probably a Commercial vehicle;</i> <i>Likely a Freight transport;</i> <i>Most likely semi trailer truck which is a large truck with a long, rectangular flatbed trailer;</i> <i>Probably truck which has large, boxy vehicle.</i>
(1) Ground-truth: Horse		(2) Ground-truth: Truck	
	<i>Most likely a Peafow;</i> <i>Probably a Cassowary;</i> <i>Likely a Ostrich;</i> <i>Most likely emu which has long tail feathers;</i> <i>Probably peafowl which has long tail feathers.</i>		<i>Most likely a Pronghorn;</i> <i>Probably a Mountain goat;</i> <i>Likely a Barren ground Caribou;</i> <i>Most likely elk which has white rump patch;</i> <i>Probably elk which has long, black tail.</i>
(3) Ground-truth: Bird		(4) Ground-truth: Deer	

(b) Examples in CIFAR-10

Images	Selected Tags & Attributes	Images	Selected Tags & Attributes
	<i>Most likely a Tench;</i> <i>Probably a Giant carp;</i> <i>Likely a Common carp;</i> <i>Most likely tench which has rounded and deepyscaled body;</i> <i>Probably tench which has barbels around the mouth.</i>		<i>Most likely a Toilet paper;</i> <i>Probably a Toilet tissue;</i> <i>Likely a Toilet roll holder;</i> <i>Most likely toilet paper which often with a plastic or paper wrapper;</i> <i>Probably toilet paper which has usually has a printed design or logo.</i>
(1) Ground-truth: Tench		(2) Ground-truth: Toilet_tissue	
	<i>Most likely a Tiger shark;</i> <i>Probably a Great white shark;</i> <i>Likely a Bull shark;</i> <i>Most likely tiger shark which has long snout;</i> <i>Probably tiger shark which has black spots and stripes.</i>		<i>Most likely a Spotted Turtle;</i> <i>Probably a Spotted salamander;</i> <i>Likely a Volcanic rock;</i> <i>Most likely spotted salamander which has black, grey, or brown body with yellowishorange spots;</i> <i>Probably spotted salamander which has webbed feet.</i>
(3) Ground-truth: Tiger_shark		(4) Ground-truth: Crampfish	

(c) Examples in ImageNet

Figure 10: Generated categorical descriptive text: representative examples in generic datasets.

**Images**



**Selected Tags & Attributes**

*Most likely a pink evening primrose;  
Probably a pink primrose;  
Likely a evening primrose;  
Most likely pink primrose which has rounded sepals;  
Probably pink primrose which has pink or white flower.*

(1) Ground-truth: Pink\_primrose



*Most likely a protea;  
Probably a king protea;  
Likely a giant protea;  
Most likely king protea which has bright pink or white petals;  
Probably king protea which has large, round flower head.*

(3) Ground-truth: King\_protea

**Images**



**Selected Tags & Attributes**

*Most likely a sweet peas;  
Probably a everlasting sweet pea;  
Likely a lathyrus sativus;  
Most likely sweet pea which has pastel colors ranging from pink, white, and purple;  
Probably sweet pea which has delicate, feathery leaves.*

(2) Ground-truth: Sweet\_pea



*Most likely a daylily;  
Probably a dwarf day lily;  
Likely a stargazer lily;  
Most likely lillie which is a single pistil in the center;  
Probably peruvian lily which has dark spots on the petals.*

(4) Ground-truth: Peruvian\_lily

(a) Examples in Flowers102

**Images**



**Selected Tags & Attributes**

*Most likely a Goldfinch;  
Probably a American Goldfinch;  
Likely a Finch;  
Most likely Goldfinch which has bright yellow plumage with black and white accents;  
Probably American goldfinch which has yellow, black, and white feathers.*

(1) Ground-truth: American\_Goldfinch



*Most likely a gull;  
Probably a seagull;  
Likely a Herring Gull;  
Most likely gull which has hooked bill;  
Probably franklins gull which has orange legs and bill.*

(3) Ground-truth: California\_Gull

**Images**



**Selected Tags & Attributes**

*Most likely a Horned Grebe;  
Probably a Common Loon;  
Likely a Red necked Grebe;  
Most likely clarks grebe which has yellow eyes;  
Probably horned grebe which has Hornlike projections on either side of the head.*

(2) Ground-truth: Horned\_Grebe



*Most likely a seabird;  
Probably a albatross;  
Likely a shorebird;  
Most likely seabird which has sharp eyesight;  
Probably seabird which has streamlined body.*

(4) Ground-truth: Sooty\_Albatross

(b) Examples in CUB

**Images**



**Selected Tags & Attributes**

*Most likely a Abyssinian;  
Probably a Chausie;  
Likely a Arabian mau;  
Most likely Abyssinian which has short, soft coat;  
Probably Abyssinian which has mediumsized cat.*

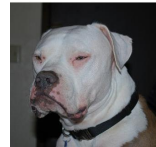
(1) Ground-truth: Abyssinian



*Most likely a Birman;  
Probably a Ragdoll cat;  
Likely a Siamese cat;  
Most likely Birman which has pointed ears;  
Probably Birman which has long, silky fur.*

(3) Ground-truth: Birman

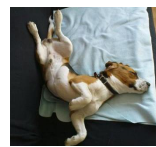
**Images**



**Selected Tags & Attributes**

*Most likely a American bulldog;  
Probably a Pit bull;  
Likely a Old english bulldog;  
Most likely American bulldog which has muscular, stocky builds;  
Probably American bulldog which has short, broad muzzle.*

(2) Ground-truth: American\_Bulldog



*Most likely a Jack russell terrier;  
Probably a Russell terrier;  
Likely a Dog bed;  
Most likely basenji which has curled tail;  
Probably treeing walker coonhound which has webbed toes.*

(4) Ground-truth: Beagle\_dog

(c) Examples in Oxford Pets

**Images**



**Selected Tags & Attributes**

*Most likely a Audi TT;  
Probably a Audi TT Hatchback 2011;  
Likely a Audi TTS Coupe 2012;  
Most likely Audi TTS coupe 2012 which has tinted windows;  
Probably Audi TT Hatchback 2011 which has two doors.*

(1) Ground-truth: Audi TTS Coupe 2012



*Most likely a Dodge Dakota;  
Probably a Dodge Dakota Club Cab 2007;  
Likely a Dodge Dakota Crew Cab 2010;  
Most likely Dodge Dakota Club Cab 2007 which is alloy wheels;  
Probably Dodge Dakota Club Cab 2007 which has rounded hood and grille.*

(3) Ground-truth: Dodge Dakota Club Cab 2007

**Images**



**Selected Tags & Attributes**

*Most likely a Acura TL;  
Probably a Acura;  
Likely a Acura TL Sedan 2012;  
Most likely Acura TL sedan 2012 which has chrome accents;  
Probably Acura TL sedan 2012 which is alloy wheels.*

(2) Ground-truth: Acura TL Sedan 2012



*Most likely a Mazda mx 3;  
Probably a Honda integra;  
Likely a Honda prelude;  
Most likely Geo Metro Convertible 1993 which has twotone paint job;  
Probably Geo Metro Convertible 1993 which has short wheelbase.*

(4) Ground-truth: Geo Metro Convertible 1993

(d) Examples in Stanford Cars

Figure 11: Generated categorical descriptive text: representative examples in fine-grained datasets.

## References

- Mahmoud Assran, Mathilde Caron, Ishan Misra, Piotr Bojanowski, Florian Bordes, Pascal Vincent, Armand Joulin, Mike Rabbat, and Nicolas Ballas. Masked siamese networks for label-efficient learning. In *European Conference on Computer Vision*, 2022.
- William Berrios, Gautam Mittal, Tristan Thrush, Douwe Kiela, and Amanpreet Singh. Towards language models that can see: Computer vision through the lens of natural language. *arXiv preprint arXiv:2306.16410*, 2023.
- Lukas Bossard, Matthieu Guillaumin, and Luc Van Gool. Food-101—mining discriminative components with random forests. In *European Conference on Computer Vision*, 2014.
- Tom Brown, Benjamin Mann, Nick Ryder, Melanie Subbiah, Jared D Kaplan, Prafulla Dhariwal, Arvind Neelakantan, Pranav Shyam, Girish Sastry, Amanda Askell, et al. Language models are few-shot learners. *Advances in Neural Information Processing Systems*, 2020.
- Mathilde Caron, Hugo Touvron, Ishan Misra, Hervé Jégou, Julien Mairal, Piotr Bojanowski, and Armand Joulin. Emerging properties in self-supervised vision transformers. In *Proceedings of the IEEE/CVF International Conference on Computer Vision*, 2021.
- Yingyi Chen, Xi Shen, Shell Xu Hu, and Johan AK Suykens. Boosting co-teaching with compression regularization for label noise. In *Proceedings of the IEEE/CVF Conference on Computer Vision and Pattern Recognition*, 2021.
- Mircea Cimpoi, Subhransu Maji, Iasonas Kokkinos, Sammy Mohamed, and Andrea Vedaldi. Describing textures in the wild. In *Proceedings of the IEEE/CVF Conference on Computer Vision and Pattern Recognition*, 2014.
- Jia Deng, Wei Dong, Richard Socher, Li-Jia Li, Kai Li, and Li Fei-Fei. Imagenet: A large-scale hierarchical image database. In *Proceedings of the IEEE/CVF International Conference on Computer Vision*, 2009.
- Alexey Dosovitskiy, Lucas Beyer, Alexander Kolesnikov, Dirk Weissenborn, Xiaohua Zhai, Thomas Unterthiner, Mostafa Dehghani, Matthias Minderer, Georg Heigold, Sylvain Gelly, et al. An image is worth 16x16 words: Transformers for image recognition at scale. *arXiv preprint arXiv:2010.11929*, 2020.
- Agrim Gupta, Piotr Dollar, and Ross Girshick. Lvis: A dataset for large vocabulary instance segmentation. In *Proceedings of the IEEE/CVF Conference on Computer Vision and Pattern Recognition*, 2019.
- Bo Han, Quanming Yao, Xingrui Yu, Gang Niu, Miao Xu, Weihua Hu, Ivor Tsang, and Masashi Sugiyama. Co-teaching: Robust training of deep neural networks with extremely noisy labels. *Advances in Neural Information Processing Systems*, 2018.
- Jonathan Krause, Michael Stark, Jia Deng, and Li Fei-Fei. 3d object representations for fine-grained categorization. In *Proceedings of the IEEE/CVF International Conference on Computer Vision Workshops*, 2013a.
- Jonathan Krause, Michael Stark, Jia Deng, and Li Fei-Fei. 3d object representations for fine-grained categorization. In *Proceedings of the IEEE/CVF International Conference on Computer Vision Workshops*, 2013b.

- Ranjay Krishna, Yuke Zhu, Oliver Groth, Justin Johnson, Kenji Hata, Joshua Kravitz, Stephanie Chen, Yannis Kalantidis, Li-Jia Li, David A Shamma, et al. Visual genome: Connecting language and vision using crowdsourced dense image annotations. *International Journal of Computer Vision*, 2017.
- Alex Krizhevsky, Geoffrey Hinton, et al. Learning multiple layers of features from tiny images. *Technical Report*, 2009.
- Alina Kuznetsova, Hassan Rom, Neil Alldrin, Jasper Uijlings, Ivan Krasin, Jordi Pont-Tuset, Shahab Kamali, Stefan Popov, Matteo Mallocci, Alexander Kolesnikov, et al. The open images dataset v4: Unified image classification, object detection, and visual relationship detection at scale. *International Journal of Computer Vision*, 2020.
- Fei-Fei Li, Marco Andreto, Marc’Aurelio Ranzato, and Pietro Perona. Caltech 101, 2022a.
- Junnan Li, Dongxu Li, Caiming Xiong, and Steven Hoi. Blip: Bootstrapping language-image pre-training for unified vision-language understanding and generation. In *International Conference on Machine Learning*, 2022b.
- Junnan Li, Dongxu Li, Silvio Savarese, and Steven Hoi. Blip-2: Bootstrapping language-image pre-training with frozen image encoders and large language models. *arXiv preprint arXiv:2301.12597*, 2023a.
- Yanghao Li, Haoqi Fan, Ronghang Hu, Christoph Feichtenhofer, and Kaiming He. Scaling language-image pre-training via masking. In *Proceedings of the IEEE/CVF Conference on Computer Vision and Pattern Recognition*, 2023b.
- Tsung-Yi Lin, Michael Maire, Serge Belongie, James Hays, Pietro Perona, Deva Ramanan, Piotr Dollár, and C Lawrence Zitnick. Microsoft coco: Common objects in context. In *European Conference on Computer Vision*, 2014.
- James MacQueen et al. Some methods for classification and analysis of multivariate observations. In *Proceedings of the Fifth Berkeley Symposium on Mathematical Statistics and Probability*, 1967.
- Subhransu Maji, Esa Rahtu, Juho Kannala, Matthew Blaschko, and Andrea Vedaldi. Fine-grained visual classification of aircraft. *arXiv preprint arXiv:1306.5151*, 2013.
- Sachit Menon and Carl Vondrick. Visual classification via description from large language models. *arXiv preprint arXiv:2210.07183*, 2022.
- Maria-Elena Nilsback and Andrew Zisserman. Automated flower classification over a large number of classes. In *2008 Sixth Indian Conference on Computer Vision, Graphics & Image Processing*, 2008.
- Zachary Novack, Julian McAuley, Zachary Chase Lipton, and Saurabh Garg. Chils: Zero-shot image classification with hierarchical label sets. In *International Conference on Machine Learning*. PMLR, 2023.
- Rabah Ouldnooghi, Chia-Wen Kuo, and Zsolt Kira. Clip-gcd: Simple language guided generalized category discovery. *arXiv preprint arXiv:2305.10420*, 2023.
- Omkar M Parkhi, Andrea Vedaldi, Andrew Zisserman, and CV Jawahar. Cats and dogs. In *Proceedings of the IEEE/CVF Conference on Computer Vision and Pattern Recognition*, 2012.
- Nan Pu, Zhun Zhong, and Nicu Sebe. Dynamic conceptional contrastive learning for generalized category discovery. In *Proceedings of the IEEE/CVF Conference on Computer Vision and Pattern Recognition*, 2023.

- Alec Radford, Jong Wook Kim, Chris Hallacy, Aditya Ramesh, Gabriel Goh, Sandhini Agarwal, Girish Sastry, Amanda Askell, Pamela Mishkin, Jack Clark, et al. Learning transferable visual models from natural language supervision. In *International Conference on Machine Learning*, 2021.
- Subhankar Roy, Evgeny Krivosheev, Zhun Zhong, Nicu Sebe, and Elisa Ricci. Curriculum graph co-teaching for multi-target domain adaptation. In *Proceedings of the IEEE/CVF conference on computer vision and pattern recognition*, 2021.
- Olga Russakovsky, Jia Deng, Hao Su, Jonathan Krause, Sanjeev Satheesh, Sean Ma, Zhiheng Huang, Andrej Karpathy, Aditya Khosla, Michael Bernstein, et al. Imagenet large scale visual recognition challenge. *International Journal of Computer Vision*, 2015.
- Vladimir M Sloutsky. From perceptual categories to concepts: What develops? *Cognitive science*, 2010.
- Kiat Chuan Tan, Yulong Liu, Barbara Ambrose, Melissa Tulig, and Serge Belongie. The herbarium challenge 2019 dataset. *arXiv preprint arXiv:1906.05372*, 2019.
- Sagar Vaze, Kai Han, Andrea Vedaldi, and Andrew Zisserman. Generalized category discovery. In *Proceedings of the IEEE/CVF Conference on Computer Vision and Pattern Recognition*, 2022.
- Catherine Wah, Steve Branson, Peter Welinder, Pietro Perona, and Serge Belongie. The caltech-ucsd birds-200-2011 dataset. *Computation & Neural Systems Technical Report*, 2011.
- Hongjun Wang, Sagar Vaze, and Kai Han. Sptnet: An efficient alternative framework for generalized category discovery with spatial prompt tuning. In *The Twelfth International Conference on Learning Representations*, 2023.
- Hongxin Wei, Lei Feng, Xiangyu Chen, and Bo An. Combating noisy labels by agreement: A joint training method with co-regularization. In *Proceedings of the IEEE/CVF conference on computer vision and pattern recognition*, 2020.
- Xin Wen, Bingchen Zhao, and Xiaojuan Qi. Parametric classification for generalized category discovery: A baseline study. In *Proceedings of the IEEE/CVF International Conference on Computer Vision*, 2023.
- Jianxiong Xiao, James Hays, Krista A Ehinger, Aude Oliva, and Antonio Torralba. Sun database: Large-scale scene recognition from abbey to zoo. In *Proceedings of the IEEE/CVF Conference on Computer Vision and Pattern Recognition*, 2010.
- Fengxiang Yang, Ke Li, Zhun Zhong, Zhiming Luo, Xing Sun, Hao Cheng, Xiaowei Guo, Feiyue Huang, Rongrong Ji, and Shaozi Li. Asymmetric co-teaching for unsupervised cross-domain person re-identification. In *Proceedings of the AAAI conference on artificial intelligence*, 2020.
- Yue Yang, Artemis Panagopoulou, Shenghao Zhou, Daniel Jin, Chris Callison-Burch, and Mark Yatskar. Language in a bottle: Language model guided concept bottlenecks for interpretable image classification. In *Proceedings of the IEEE/CVF Conference on Computer Vision and Pattern Recognition*, 2023.
- Jiahui Yu, Zirui Wang, Vijay Vasudevan, Legg Yeung, Mojtaba Seyedhosseini, and Yonghui Wu. Coca: Contrastive captioners are image-text foundation models. *arXiv preprint arXiv:2205.01917*, 2022.
- Ye Yuan, Can Sam Chen, Zixuan Liu, Willie Neiswanger, and Xue Steve Liu. Importance-aware co-teaching for offline model-based optimization. *Advances in Neural Information Processing Systems*, 2024.

Sheng Zhang, Salman Khan, Zhiqiang Shen, Muzammal Naseer, Guangyi Chen, and Fahad Shahbaz Khan. Promptcal: Contrastive affinity learning via auxiliary prompts for generalized novel category discovery. In *Proceedings of the IEEE/CVF Conference on Computer Vision and Pattern Recognition*, 2023.

Bingchen Zhao, Xin Wen, and Kai Han. Learning semi-supervised gaussian mixture models for generalized category discovery. *arXiv preprint arXiv:2305.06144*, 2023.